CHAPTER IV
DEVELOPMENT OF POLYDIPHENYLAMINE/ZEOLITE Y COMPOSITE BY DEALUMINATION PROCESS AS A SENSING MATERIAL FOR HALOGENATED SOLVENTS

4.1 Abstract

Polydiphenylamine and zeolite Y composite were fabricated and tested for the ability to detect the halogenated solvent vapors: dichloromethane, 1,2-dichloroethane, and chloroform. To enhance the sensing properties of the composites, zeolite Y was modified by the dealumination process. The sensitivity of the composites towards the halogenated solvents was examined under the effects of acid treatment time, zeolite content, temporal response, and cyclic response. The resultant dealuminated zeolite Y showed a higher sensitivity than the pristine zeolite when exposed to solvents. An acid treatment time of 12 hr provided the highest sensitivity. Sensitivity of the composites towards dichloromethane was higher than those of 1,2-dichloroethane, and chloroform, respectively. The optimal dealuminated zeolite content in the composite was 30 %v/v.

Keywords: Conducting polymers; Polydiphenylamine; Zeolites; Sensors; Dealumination process; Halogenated hydrocarbon

4.2 Introduction

Halogenated hydrocarbons are widely used for many industrial purposes. They are used in the productions of herbicides, plastics, and solvents; solvent degreasing in the automotive and aerospace industries; dry-solvent cleaning; and solvent cleaning in the electronic field (US EPA, 1991; Sidebottom and Frankiln, 1996). However, halogenated hydrocarbons impose several environmental problems, and exhibit high toxicity towards humans (Vallero *et al.*, 1994). In order to reduce the risks of these problems, highly responsive chemical gas sensors are required to identify and detect toxic halogenated hydrocarbon vapors. Sensing materials

previously investigated have been identified to contain a conductive polymer as a base material (Bai and Shi, 2007; Shamloo *et al.*, 2012; Das and Prusty, 2012) and a porous material as a selective material (Sahner *et al.*, 2008).

Polydiphenylamine, PDPA, is a conductive polymer which is quite robust, high thermal and environmental stability, stable in a greater pH range than polyaniline, as well as and an inexpensive monomer (Agbor *et al.*, 1995). Moreover, PDPA has been used as a material for many sensory systems such as methanol sensors (Permpool *et al.*, 2012), Fe^{3-} ion sensors (Suganandam *et al.*, 2005), optical pH sensors (Tsai *et al.*, 2003), ascorbic acid sensors (Ragupathy *et al.*, 2009), ammonia sensors (Gopalan *et al.*, 2006), and carbon monoxide sensors (Santhosh *et al.*, 2007).

Zeolites are well known as micro porous materials and are widely used in many applications such as a catalyst for water purification (Shobaky *et al.*, 1979), catalyst for ethylene oligomerization to liquid fuels (Saidina and Anggoro, 2002), gas separation membrane for fuel cells (Adjemian *et al.*, 2002; Antonucci *et al.*, 1999), absorbent in refrigerators (Miguel and Manfred, 2003), and sensor applications (Chuapradit *et al.*, 2005; Densakulprasert *et al.*, 2005; Meier *et al.*, 1995; Payra and Dutta, 2003; Xie *et al.*, 2005). Their unique properties are high surface area and porosity, shape selectivity, controllable acidity, adsorptivity, and presence of mobile ions (Sahner *et al.*, 2008; Corma, 1995; Dong *et al.*, 2002; Maxwell *et al.*, 2001; Valkenberg and Holderich, 2002). These zeolite properties can be controlled by varying the Si/Al ratio. The dealumination method is a method to remove aluminum from the framework resulting in a higher Si/Al ratio, chemical and thermal stabililty, and zeolite hydrophobicity (Saidina and Anggoro, 2002; Holmberg *et al.*, 2004; Kumar *et al.*, 2000; Triantafillidis *et al.*, 2000).

In this work, doped polydiphenylamine (D-PDPA) was used as a base material and zeolite Y, Si/Al = 80 (YH[80]) as a selective material to make up the composites to be used as sensing materials for detecting the halogenated solvents dichloromethane (DCM), 1,2-dichloroethane (DCE), and chloroform. In order to improve the sensitivity of the composites towards these halogenated solvents, zeolite Y was modified by the acid treatment-dealumination process to increase the Si/Al ratio. The composition and structure characterization of dealuminated zeolite Y

(DYH) was investigated. The effects of acid treatment time, zeolite content, cyclic response, and chemical interaction of the composite were also investigated. As for PDPA, it is doped with a hydrochloric acid solution at the doping mole ratio of 100:1 ($N_{HCl}/N_{monomer}$).

4.3 Experimental

4.3.1 Materials

Diphenylamine, DPA (reagent, Sigma Aldrich), ammonium persulfate, $(NH_4)_2S_2O_8$, (AR grade, Riedel-de Haën), 36.5-38.0 %w/w of hydrochloric acid at the mole ratio of 100:1 (N_{HCl}:$N_{monomer}$), HCl, (ACS reagent, J.T. Baker) were used for the D-PDPA synthesis. Zeolite Y (Zeolite International) with H^+ as a cation, possesses the Si/Al ratio of 80 (YH[80]) in powder form. Ammonium hydroxide, NH_4OH, (AR grade, Panreac), toluene (AR grade, Panreac), isopropyl alcohol (AR grade, Burdick & Jackson), and ethanol (AR grade, Lab Scan) were used without further purification.

4.3.2 Synthesis of Polydiphenylamine

The Chemical oxidative polymerization was used to synthesize PDPA (Zhao *et al.*, 2005). The DPA monomers in toluene were mixed with a 1 M HCl solution. The solution was stirred for 15 min. After that, the $(NH_4)_2S_2O_8$ solution was added and stirred continuously at 0 °C for 4 hr. The resultant green slurry of PDPA was washed with isopropanol and filtered. Then, PDPA was neutralized by immersing in NH_4OH at the ratio of 1:3 to get rid of an excess hydrochloric acid. After that, PDPA was doped with HCl at the ratio of 1:100 (N_{DPA}:N_{HCl}).

4.3.3 Dealumination of Zeolite Y

The pristine YH[80] (supplied from Zeolyst International, with hydrogen cation) went through an acid treatment process (Holmberg *et al.*, 2004). The pristine YH[80] was treated with 1M HCl solution at 90 °C by varying the acid treatment times (2, 4, 8, 10, 12, 18, and 24 hr) to obtain various Si/Al ratios. In the

dealumination process, all samples were filtered and washed with distilled water at least 3 times.

4.3.4 Preparation of D-PDPA/DYH[80] Composites

The composites of D-PDPA and DYH[80] were prepared as a circular pellet (1 cm in diameter) by a hydraulic press (GRASEBY SPECAC) at a pressure between 4 tons - 5 tons. The D-PDPA was mixed with DYH[80] at various zeolite Y contents (0, 5, 10, 15, 20, 25, 30, 35, and 40 %v/v). A digital thickness gauge (PEAACOCK, model PDN-20) was used to measure the thickness of each composite.

4.3.5 Composition & Structure Characterization

The Fourier transform infrared (FT-IR) spectra of the samples were recorded with a Thermo Nicolet FT-IR spectrometer; model Nexus 670 in a wave number range of 1600-400 cm^{-1}, a resolution of 4 cm^{-1}, and a scan number of 64. The silicon and aluminum content were measured by an AXIOS, PW440, X-ray fluorescence (XRF). The morphology and crystal size of the samples were investigated by a HITACHI, S-4800 scanning electron microscope (SEM) with a magnification of 10,000x, operated at 10 kV. The Brunauer-Emmett-Teller (BET) surface area of the samples was measured by a Thermo Finnigan, Sorptomatic 1990 surface area analyzer (SAA). The samples were weighed and out gassed at 300 °C for 12 hr before determination of the adsorption and desorption isotherms with the He and N_2 gases. The temperature program of the sample was measured by a Perkin Elmer, TGA7, thermo gravimetric analyzer (TGA). The experiment was carried out by weighing a powder sample of 5 mg to 10 mg with a heating rate 10 °C/min from 30 °C - 900 °C. The charges distribution along the composite backbone was measured by an electrostatic force microscopy (EFM) (Park System, XE-100) operating in the standard EFM mode with an NSC 14/Cr-Au tip, a scan size of 1μm × 1μm, and a scan rate of 0.1 Hz. The voltage was applied to the sample at 5V. The EFM phase image exhibited brighter regions as the positively charges within the composite respond to the applied voltage. The EFM phase image exhibited darker

regions as the negatively charges within the composite respond to the applied voltage.

4.3.6 Conductivity and Sensitivity Measurements

The conductivity and sensitivity of all samples towards the halogenated solvents were measured by the two point probe method. The probes were connected to a KEITHLEY 6517A conductivity meter and the current was measured in response to the applied voltage. The electrical conductivity of the samples was calculated by Eq. (4.1):

$$\sigma = (I/KVt) \qquad (4.1)$$

where I is the measured current (A), V is the applied voltage (V), t is the thickness of samples, and K is the geometric correction factor that was calibrated by using standard silicon wafer sheets with known specific resistivity values. The change in conductivity of all samples ($\Delta\sigma/\sigma_{N2,\ initial}$) when exposed to a halogenated solvent divided by the conductivity in pure nitrogen is defined as the sensitivity. The difference in the specific electrical conductivity (S/cm) is $\Delta\sigma$ and it was calculated by Eq. (4.2):

$$\Delta\sigma = \sigma_{halogenated\ solvents} - \sigma_{N2,\ initial} \qquad (4.2)$$

where $\sigma_{N2,\ initial}$ is the specific electrical conductivity in N_2 before the exposure (S/cm), and $\sigma_{halogenated\ solvent}$ is the specific electrical conductivity (S/cm) under the halogenated solvent exposure at various concentrations. All measurements were taken at 27 ± 1 °C, at the atmospheric pressure using a 5 L/min air and N_2 flow rate.

4.4 Results and Discussion

4.4.1 Composition and Structure of Dealuminated Zeolite Y

The FT-IR spectra of the YH[80] are shown in Figure 4.1a. The absorption band at 3385 and 1207, 1081 cm^{-1} and can be assigned to the SiO_4, and AlO_4, vibrations, respectively (Titova *et al.*, 1993). The absorption bands at 832, 611, 526, and 459 cm^{-1} can be assigned to the vibrations of Si-O-Al bonds (Titova *et al.*, 1993). For the dealuminated zeolite Y (DYH[80]) through varying an acid treatment time, the intensity of the absorption band at 1081 cm^{-1} decreases with increasing acid treatment time (Triantafillidis *et al.*, 2000). This is due to the lower aluminum content within the zeolite framework (Shirazi *et al.*, 2008). Figure 4.1b shows an example of FT-IR spectra of DYH[80] at 2 hr and 4 hr acid treatment times, and the areas under the bands were calculated by using a curve fitting technique (Saidina and Anggoro, 2002). The calculated band areas of the AlO_4 (1081 cm^{-1}) of the dealuminated samples were compared with the integrated band area of the vibrations of the Si-O-Al bonds (832 cm^{-1}) which do not change with the acid treatment time (internal standard). The resultant integrated band area decreases in the following order: 0>2>4>8>10>12 hr, as shown in Table 4.1. The actual Si/Al contents of DYH[80] are also given in Table 4.1. The Si/Al ratio increases with increasing acid treatment time (Shirazi *et al.*, 2008); it increases from 61.58 to 263.34 when acid treatment time increases from 2 hr to 12 hr. For the increase in the acid treatment time from 18 hr to 24 hr, the Si/Al ratio decreases to 142.73. This is a result of the long dealumination process. The zeolite framework is destroyed, a result which is in agreement with Triantafillidis and co-workers (Triantafillidis *et al.*, 2000). They modified zeolite Y using different dealumination processes to study the influence of the degree and type of dealumination on the structure and acidicity of zeolite Y. They found that after hydrothermal dealumination, agglomeration of the particles occurred. This was because the hydroxyl groups at the surface bonded with neighboring crystallites. The surface areas of the present samples are tabulated in Table 4.1. The surface area increases with increasing acid treatment time (Shirazi *et al.*, 2008) from 683.78 m^2/g to 930.58 m^2/g, when acid treatment time increases from 2 hr to 12 hr, and decreases to 542.10 m^2/g when the acid treatment time is between 18 hrs and 24

hrs. The morphology of DYH[80] is the same as YH[80] (Figure 4.2), but the crystal size decreases with increasing acid treatment time in the range from 1.138 μm to 0.670 μm (Shirazi *et al.*, 2008). The TGA thermograms are shown in Figure 4.3. The weight loss, in the temperature range of 50-100 °C can be attributed to the water loss and it decreases with increasing acid treatment time. This is due to the fact that a higher acid treatment time provides more hydrophobicity to DYH[80]. Therefore, the lower aluminum content in the zeolite structure, the lower water present in the zeolite structure. The weight loss between 500-700 °C is due to the thermal dehydroxylation of hydroxyl nests site (Si-OH) of DYH[80] (Beyer, 2002; Shough, 2008). Hence, the water content in the structure of DYH[80] at a high Si/Al ratio has a lower value than that at a low Si/Al ratio (Shirazi, 2008; Xia *et al.*, 2008).

4.4.2 Effect of Acid Treatment Times on the Sensitivity towards Halogenated Solvents

Figure 4.4 shows the sensitivity values of YH[80] and DYH[80] in relation to the acid treatment time under exposure to DCM, DCE, and chloroform. The sensitivity of Y H 80 is $(-1.20 \pm 0.44) \times 10^{-1}$, $(-6.27 \pm 0.71) \times 10^{-2}$, and $(-7.13 \pm 0.34) \times 10^{-2}$ for DCM, DCE, and chloroform, respectively. When the acid treatment time increases from 2 hrs to 12 hrs, the sensitivity of DYH[80] increases from $(-1.21 \pm 0.90) \times 10^{-1}$ to $(-5.63 \pm 3.45) \times 10^{-1}$, from $(-3.30 \pm 0.75) \times 10^{-2}$ to $(-1.07 \pm 0.03) \times 10^{-1}$, and from $(-1.37 \pm 0.19) \times 10^{-2}$ to $(-7.29 \pm 0.44) \times 10^{-2}$ for DCM, DCE, and chloroform, respectively. When the acid treatment time increases from 18 hr to 24 hr, the sensitivity decreases to $(-3.62 \pm 0.48) \times 10^{-1}$, $(-6.41 \pm 4.59) \times 10^{-2}$, and $(-5.79 \pm 1.45) \times 10^{-2}$ for DCM, DCE, and chloroform, respectively (Table 4.2). The sensitivity of DYH[80] is higher than the sensitivity of YH[80] and increases with increasing acid treatment time from 2 hr to 12 hr. The dealumination process removes aluminum from the zeolite framework causing more hydrogen atoms in the framework structure; the mechanism is shown in Figure 4.5 (González *et al.*, 2011). Hence, DYH[80] has more hydrogen atoms available to induce hydrogen bonding with the solvent molecules than YH[80] (Ayad *et al.*, 2008; Shukla *et al.*, 2011; Vijayakumar *et al.*, 2012). Among the solvents, DCM has the highest sensitivity followed by DCE, then chloroform. The reason for this phenomenon is same as in

the above discussion: the higher the hydrogen bonding with solvent molecules, the higher the sensitivity of the zeolite (Cangelosi and Shaw, 1983). DCM has two hydrogen atoms in its molecule; it can form two hydrogen bonds per molecule with DYH[80]. DCE has two hydrogen atoms in its molecule, the same as DCM, but DCE has a large molecule than DCM. So, the sensitivity of DYH[80] toward DCE is lower than DCM due to the steric effect. The chloroform molecule has one hydrogen atom; it can form only one hydrogen bond with the zeolite structure. Therefore, the sensitivity of DYH[80] toward chloroform is relatively low. Furthermore, the decrease in sensitivity of D Y H 80 with an increase of the acid treatment time from 18 hrs to 24 hrs could be related to the excessive dealumination time. The zeolite structure was destroyed (Triantafillidis *et al.*, 2000). The acid treatment time of 12 hr thus provided the highest sensitivity towards all of the solvents. This condition was then used for fabrication of the composites between D-PDPA and DYH[80] (D-PDPA/DYH[80](12h)).

4.4.3 Effect of Zeolite Content in the Composites on the Sensitivity towards Halogenated Solvents

The effect of DYH[80](12h) content on the sensitivity of the composites towards the solvents is examined next. Figure 4.6 shows the sensitivity of D-PDPA/DYH[80](12h) composites towards DCM, DCE, and chloroform in relation to the D Y H 80(12h) content. The sensitivity of D-PDPA is $(-5.50 \pm 3.30) \times 10^{-2}$, $(-6.26 \pm 3.70) \times 10^{-2}$, and $(-1.22 \pm 0.16) \times 10^{-3}$ towards DCM, DCE, and chloroform, respectively. For the composites, as the zeolite content varies from 5 %v/v to 30 %v/v, the sensitivity of the composites increases from $(-1.51 \pm 0.12) \times 10^{-1}$ to $(-4.44 \pm 0.10) \times 10^{-1}$, from $(-4.87 \pm 0.65) \times 10^{-2}$ to $(-2.01 \pm 0.25) \times 10^{-1}$, and from $(-1.04 \pm 0.03) \times 10^{-2}$ to $(-9.07 \pm 3.95) \times 10^{-2}$ for DCM, DCE, and chloroform, respectively. When DYH[80](12h) content increases to 40 %v/v, the sensitivity decreases to $(-2.04 \pm 0.18) \times 10^{-1}$, $(-8.64 \pm 3.88) \times 10^{-2}$, $(-7.58 \pm 2.98) \times 10^{-2}$ for DCM, DCE, and chloroform, respectively (Table 4.3). The initial increase in sensitivity of the composite with increasing zeolite content is because the zeolite has a micro-porous structure which can trap solvent molecules. Thereby, the higher the zeolite content in the composite, the more the solvent molecules can be trapped (Zheng *et al.*, 2012).

However, when the zeolite content is between 30 %v/v and 40 %v/v, the sensitivity of the composites decreases because the active site of the conductive polymer decreases (Phumman *et al.*, 2009). The differences in the sensitivity of the composites can be traced back to the interaction between the composites and the vapors. The interaction between D-PDPA and the vapors is the dipole-dipole interaction of hydrogen atoms in the vapor molecule and the positive charges on the imine N_2 in the quinine ring, similar to the interaction between D-PDPA and N_2; but the vapor interaction is stronger (Thuwachaowsoan *et al.*, 2007). Due to the strong dipole-dipole interaction between D-PDPA and the vapors, electrons on the polymer chain tend to move slower. This results in a negative sensitivity response in the composites relative to those of N_2. The interaction between DYH[80] and the vapors is the physical adsorption of the vapor molecules in the zeolite framework. The hydrogen atom can interact with –OH in the DYH[80]. With more –OH in the zeolite, the interaction between the vapors and the zeolite increases. This results in an increase in the sensitivity of the composites. It appears that the differences in the sensitivity values of the composites towards the solvents can be attributed to the change in the Si/Al ratio of the zeolite via the dealumination process.

Figure 4.7 shows the sensitivity values of the composites D-PDPA with zeolite Y with and without dealumination process in relation to the zeolite content towards DCM, DCE, and chloroform. For the composite with YH[80], the sensitivity varies from $(-1.16 \pm 0.08) \times 10^{-1}$ to $(-3.48 \pm 1.64) \times 10^{-1}$ for DCM, from $(-2.90 \pm 0.03) \times 10^{-2}$ to $(-1.77 \pm 0.04) \times 10^{-1}$ for DCE, and from $(-9.27 \pm 0.77) \times 10^{-3}$ to $(-3.95 \pm 1.86) \times 10^{-2}$ for chloroform, as the zeolite content increases from 5 %v/v to 30 %v/v. For the composite with DYH[80](12h), the sensitivity varies from $(-1.51 \pm 0.12) \times 10^{-1}$ to $(-4.44 \pm 0.10) \times 10^{-1}$ for DCM, from $(-4.87 \pm 0.65) \times 10^{-2}$ to $(-2.01 \pm 0.25) \times 10^{-1}$ for DCE, and from $(-1.04 \pm 0.03) \times 10^{-2}$ to $(-9.07 \pm 3.95) \times 10^{-2}$ for chloroform as zeolite content increases from 5 %v/v to 30 %v/v. Thus the higher sensitivity values of the composites with DYH[80] towards all of the solvents can be observed as more vapor molecules can be absorbed into the dealuminated zeolite.

4.4.4 The Temporal Response of D-PDPA/DYH[80](12h) Composites

The induction time is the time interval when electrical conductivity of the samples reaches equilibrium after being exposed to the vapors (Thuwachaowsoan *et al.*, 2007). Table 4.4 shows the induction time of YH[80] is 15.42 ± 0.11, 9.45 ± 0.14, and 6.45 ± 0.57 min for DCM, DCE, and chloroform, respectively. For DYH[80], the induction time increases from 14.62 ± 0.23 min to 17.61 ± 0.09 min, from 9.35 ± 0.42 min to 12.51 ± 0.23 min, and from 7.40 min ± 0.21 to 10.33 ± 0.46 min for DCM, DCE, and chloroform, respectively as acid treatment time increases from 2 hrs to 12 hrs. As the acid treatment time increases from 18 hrs to 24 hrs, it decreases to 15.56 ± 0.01, 11.25 ± 0.29, and 9.48 ± 0.25 min for DCM, DCE, and chloroform, respectively. The induction time of DYH[80](12h) is higher than the induction time of YH[80] and it increases with increasing acid treatment times because as the acid treatment time increases, this leads to the increase in –OH bonding within the zeolite structure (Figure 4.5). So, DYH[80] has more active sites available for the solvent molecules to absorb. It takes a longer time to reach equilibrium. The higher the Si/Al ratio, the longer the time required to reach equilibrium.

The induction time of D-PDPA is 11.35 ± 0.21 min, 8.01 ± 0.63 min, and 7.74 ± 0.34 min for DCM, DCE, and chloroform, respectively (Table 4.4). For the composites, the induction time increases from 12.48 ± 0.04 min to 15.50 ± 0.07 min, from 10.48 ± 0.25 min to 12.81 ± 0.23 min, and from 10.17 ± 0.07 min to 13.66 ± 0.30 min for DCM, DCE, and chloroform, respectively as zeolite content increases from 5 %v/v to 30 %v/v. When the zeolite content increases to 40 %v/v, it decreases to 14.45 ± 0.16 min, 11.67 ± 0.16 min, and 12.77 ± 0.17 min for DCM, DCE, and chloroform, respectively. When adding zeolite into D-PDPA, the induction times of the composites are higher than those of pure D-PDPA. At a higher DYH[80](12h) content, more vapor molecules can be absorbed into the composites. The optimal zeolite content is 30 %v/v and it has the longest induction time towards the solvents. Beyond this zeolite content, the induction time decreases because the active sites available on the zeolite structure to interact are lower (Phumman *et al.*, 2009).

The recovery times of all samples show the same trend as the induction time (Table 4.4). The recovery time of DYH[80] increases with increasing

zeolite content. For the composites, the recovery times of the composites are longer than that of D-PDPA and they also increase with increasing zeolite content. Furthermore, the recovery times of D-PDPA, the zeolite, and the composites towards DCM are higher than those of DCE and chloroform. This is because DCM has more hydrogen molecules to form hydrogen bonds with the active sites.

4.4.5 Effect of Vapor Concentration on the Electrical Sensitivity of the Composites towards Halogenated Solvents

Figure 4.8 shows the sensitivity of D-PDPA/30%DYH[80](12h) composite versus vapor concentration. When a composite [D-PDPA/30%DYH[80](12h)] is exposed to DCM, the sensitivity of the composite increases from $(-3.61 \pm 3.34) \times 10^{-2}$ to $(-4.42 \pm 0.01) \times 10^{-1}$ as the DCM concentration increases from 7,696 ppm to 153,914 ppm, respectively. When the composite is exposed to DCE, the sensitivity of the composite increases from $(-1.57 \pm 0.02) \times 10^{-2}$ to $(-2.01 \pm 0.02) \times 10^{-1}$ as vapor concentration increases from 1,015 ppm to 20,299 ppm, respectively. The data shows that the responses of the composite are nearly linear with respect to concentrations of the vapors. The slope of DCM vapor is greater than that of DCE vapor. This suggests that the selectivity of the composite toward DCM is higher than the selectivity toward DCE. A similar result was found in Ma *et al.* (2011). They studied the sensing properties of a triangular nano-sensor based on localized surface plasmon resonance towards ethanol, acetone, benzene, propanol, and hexane. They made the comparison of the peak wavelengths in response to the tested vapors. A good linear response was obtained. Ethanol showed the greatest slope among the tested vapors. It was concluded that the sensor has higher selectivity towards ethanol relative to other vapors. Luo *et al.* (2012) developed the sensing properties of the composite film of polyurethane and multiwall carbon nanotubes towards benzene, cyclohexane, carbontetrachloride. The response of the composites film, with the benzene and cyclohexane concentrations varied from 1,500 ppm to 7,500 ppm, increased linearly with increasing vapor concentration.

4.4.6 The Cyclic Response and Chemical Reaction of D-PDPA/30%DYH[80](12h) Composites and the Vapors

Figure 4.9 shows the electrical conductivity of D-PDPA/30%DYH[80](12h) composite versus time toward DCM. The measurement spans 3 cycles, to determine the reversibility of the electrical conductivity. The composite shows the negative cyclic response when exposed to DCM. The conductivity values of the composite of the 1st, 2nd, and 3rd cycles are 6.71×10^{-6}, 6.59×10^{-6}, and 6.54×10^{-6} S/cm, respectively. The conductivity values of the 2nd and 3rd cycle do not recover the conductivity value of the 1st cycle. This suggests that the interaction between the composites and the vapors is not reversible. Moreover, the chemical interaction between the composites and the vapors can be confirmed by using a FT-IR spectrometer. The FT-IR spectra of the composite before, during, and after the exposure to DCM are shown in Figure 4.10. Before DCM exposure, the spectrum shows only the characteristic peaks of D-PDPA and DYH[80](12h) (Santana and Dias, 2003; Hua and Ruckenstein, 2003; Sathiyanarayanan *et al.*, 2006). During DCM exposure, the new peaks occur at 3009, 1275, and 750 cm^{-1} which can be assigned to the interaction between DCM and D-PDPA; CH_2 in DCM (Lambert *et al.*, 2010); and the interaction between DCM and DYH[80], respectively (Robert *et al.*, 2005). When DCM is removed and replaced with N_2, the absorption bands at 3009 cm^{-1} disappear, but the absorption bands at 1275 and 750 cm^{-1}, which are assigned to the interaction between DCM and DYH[80], still remain. This indicates that the interaction between the composite and the vapor is irreversible. Figure 4.11 shows the proposed mechanism of the composite and DCM vapor. The chlorine atom of DCM is electron donating. It will stabilize the cation of the imines nitrogen in the composite. The electron can move along the D-PDPA backbone. This results in an increase in the conductivity of D-PDPA. On the other hand, the hydrogen atom in the DCM molecule is electron withdrawing. It removes the electron from the active site in DYH[80] (–OH) and creates a hole on the DYH[80] structure as a p type doping. The electron can move through π-bonds of the –OH, increasing the conductivity of the composite. This phenomenon is called the resonance effect (Xu *et al.*, 2002). During the dealumination process, as more active sites (-OH) of the DYH[80] are available, the greater resonance effect. Thus

conductivity increases by adding DYH[80]. In addition, the charge distribution on the surface of the composite can be observed by EFM with external electric excitation of 5 volts. The EFM images (Figure. 4.11a and b) show the charges distributions on the surfaces of the composites before and after the exposure to DCM vapor. The image would appear as a bright contrast indicating the presence of positive charges; it would appear as a dark contrast when negatively charges are present (Barisci *et al.*, 2000). Before the exposure to DCM (Figure 4.12a), the image shows mainly brighter regions since the D-PDPA backbone has many holes or positively charges along the backbone due to p type doping process of D-PDPA. During the exposure to DCM (Figure 4.12b), the image shows darker regions as the vapors donate electrons to the polymer backbone. This result suggests that as the polymer is exposed to DCM, it attains more electrons along the backbone. After flushing out the DCM vapor by N_2, the EFM image (Figure 4.12c) also shows darker regions which implies that the polymer still retains some electrons. This clearly indicates that the interaction between the polymer and the vapor is irreversible. Therefore, the EFM results show that the interaction between the composite and the vapor is irreversible.

4.5 Conclusions

This work confirms a successful attempt to increase Si/Al ratios of zeolite Y by the dealumination method. The highest Si/Al ratio obtained is 263 at the acid treatment time of 12 hrs. The composites of D-PDPA and DYH[80] were then used as a sensing material to investigate the electrical sensitivity towards three halogenated solvents; DCM, DCE, and chloroform. The composites with the dealuminated zeolite Y have a potential use as sensing materials for the halogenated solvents because they have a higher number of reactive sites in DYH[80] to react with the vapors. The acid treatment of 12 hr and 30 %v/v of zeolite provide the highest sensitivity towards the halogenated solvents. The results of the cyclic response show the interaction between the composite and the vapor is irreversible, as confirmed by FT-IR spectra and EFM images.

4.6 Acknowledgments

The authors would like to acknowledge the financial support from: the Conductive and Electroactive Polymers Research Unit of Chulalongkorn University; the Thailand Research Fund (TRF-RTA); the Royal Thai Government; and the Thailand Graduate Institute of Science and Technology (TGIST) (TGIST-01-54-011).

4.7 References

Adjemian, K.T., Lee, S.J., Srinivasan, S., Benziger, J., and Bocarsly, A.B. (2002) Silicon oxide nafion composite membranes for proton-exchange membrane fuel cell operation at 80-140 degrees C. Journal of the Electrochemical Society, 149(3), A256-A261.

Agbor, N.E., Petty, M.C., and Monkman, A.P. (1995) Polyaniline thin films for gas sensing. Sensors and Actuators B: Chemical, 28(3), 173-179.

Antonucci, P.L., Aricò, A.S., Creti, P., Ramunni, E., and Antonucci, V. (1999) Investigation of a direct methanol fuel cell based on a composite Nafion®-silica electrolyte for high temperature operation. Solid State Ionics, 125(1–4), 431-437.

Ayad, M.M., El-Hefnawey, G., and Torad, N.L. (2008) Quartz crystal microbalance sensor coated with polyaniline emeraldine base for determination of chlorinated aliphatic hydrocarbons. Sensors and Actuators B: Chemical, 134(2), 887-894.

Bai, H. and Shi, G. (2007) Gas sensors based on conducting polymers. Sensors, 7(3), 267-307.

Barisci, J.N., Stella, R., Spinks, G.M., and Wallace, G.G. (2000) Characterisation of the topography and surface potential of electrodeposited conducting polymer films using atomic force and electric force microscopies. Electrochimica Acta, 46(4), 519-531.

Beyer, H.K. (2002) Dealumination techniques for zeolites. Molecular Sieves, 3, 204-255.

Boubel, R.W., Fox, D.L., Turner, B.R., and Stern, A.C. (Eds.). (1994) Fundamentals of Air Pollution. San Diego: Academic Press.

Cangelosi, F. and Shaw, M.T. (1983) A reveiw of hydrogen bonding in solid polymers: structural relationships, analysis, and importance. Polymer-Plastics Technology and Engineering, 21(1), 13-98.

Chuapradit, C., Wannatong, L.R., Chotpattananont, D., Hiamtup, P., Sirivat, A., and Schwank, J. (2005) Polyaniline/zeolite LTA composites and electrical conductivity response towards CO. Polymer, 46(3), 947-953.

Corma, A. (1995) Inorganic solid acids and their use in acid-catalyzed hydrocarbon reactions. Chemical Reviews, 95, 559-614.

Das, T.K. and Prusty, S. (2012) Review on conducting polymers and their applications. Polymer-Plastics Technology and Engineering, 51(14), 1487-1500.

de Santana, H. and Dias, F.C. (2003) Characterization and properties of polydiphenylamine electrochemically modified by iodide species. Materials Chemistry and Physics, 82(3), 882-886.

Densakulprasert, N., Wannatong, L., Chotpattananont, D., Hiamtup, P., Sirivat, A., and Schwank, J. (2005) Electrical conductivity of polyaniline/zeolite composites and synergetic interaction with CO. Materials Science and Engineering: B, 117(3), 276-282.

Dong, A., Wang, Y., Tang, Y., Ren, N., Zhang, Y., Yue, Y., and Gao, Z. (2002) Zeolitic tissue through wood cell templating. Advanced Materials, 14(12), 926-929.

El-Shobaky, G.A., Selim, M.M., and Ezzo, E.M. (1979) Effect of water treatment on the catalytic properties of decationated zeolite. Journal of the Research Institute for Catalysis Hokkaido University.

EPA, U. (1991) Needs for eleven TRI organic chemical groups, environmental protection agency. Paper presented at Pollution Prevention Research, Washington, DC, USA.

González, M.D., Cesteros, Y., and Salagre, P. (2011) Comparison of dealumination of zeolites beta, mordenite and ZSM-5 by treatment with acid under

microwave irradiation. Microporous and Mesoporous Materials, 144(1–3), 162-170.

Gopalan, A.I., Kwang, P.L., Manian, K.M.P., Santhosh, P., Kap, D.S., and Duk, D.L. (2006) Fabrication of functional nanofibrous ammonia sensor. in Nanotechnology. Paper presented at IEEE-NANO 2006. Sixth IEEE Conference, Cincinnati, Ohio.

Holmberg, B.A., Wang, H., and Yan, Y. (2004) High silica zeolite Y nanocrystals by dealumination and direct synthesis. Microporous and Mesoporous Materials, 74(1–3), 189-198.

Hua, F. and Ruckenstein, E. (2003) Water-soluble conducting poly(ethylene oxide)-grafted polydiphenylamine synthesis through a "Graft Onto" process. Macromolecules, 36(26), 9971-9978.

Kaneyasu, K., Otsuka, K., Setoguchi, Y., Sonoda, S., Nakahara, T., Aso, I., and Nakagaichi, N. (2000) A carbon dioxide gas sensor based on solid electrolyte for air quality control. Sensors and Actuators B: Chemical, 66(1–3), 56-58.

Kumar, S., Sinha, A.K., Hegde, S.G., and Sivasanker, S. (2000) Influence of mild dealumination on physicochemical, acidic and catalytic properties of H-ZSM-5. Journal of Molecular Catalysis A: Chemical, 154(1–2), 115-120.

Lambert, J.B., Gronert, S., Shurvell, H.F., and Lightner, D. (2010) Organic Structural Spectroscopy. New Jersey: Prentice Hall PTR.

Luo, Y.L., Miao, Y., Xu, F., and Yao, Y. (2012) Novel HTPB/MWNTs-COOH PU conductive polymer composite films for detection of hazardous organic solvent vapors. Polymer-Plastics Technology and Engineering, 51(3), 290-297.

Ma, W., Yang, H., Wang, W., Gao, P., and Yao, J. (2011) Ethanol vapor sensing properties of triangular silver nanostructures based on localized surface plasmon resonance. Sensors, 11(9), 8643-8653.

Maxwell, I.E. and Stork, W.H.J. (2001) Hydrocarbon processing with zeolites. in Studies in Surface Science and Catalysis. In H.V. Bekkum, E.M. Flanigen, and P.A. Jacobs (Eds), Studies in Surface Science and Catalysis (pp. 747-8190). Rio de Janeiro: Elsevier.

Meier, B., Werner, T., Klimant, I., and Wolfbeis, O.S. (1995) Novel oxygen sensor material based on a ruthenium bipyridyl complex encapsulated in zeolite Y: dramatic differences in the efficiency of luminescence quenching by oxygen on going from surface-adsorbed to zeolite-encapsulated fluorophores. Sensors and Actuators B: Chemical, 29(1–3), 240-245.

Miguel, R., Rafael, L.E., and Manfred, J.H. (2003) Evaluation of zeolite-water solar adsorption refrigerator. Paper presented at ISES Solar World Congress, Sweden.

Payra, P. and Dutta, P.K. (2003) Development of a dissolved oxygen sensor using tris(bipyridyl) ruthenium (II) complexes entrapped in highly siliceous zeolites. Microporous and Mesoporous Materials, 64(1–3), 109-118.

Permpool, T., Supaphol, P., Sirivat, A., and Wannatong, L. (2012) Polydiphenylamine–polyethylene oxide blends as methanol sensing materials. Advances in Polymer Technology, 31(4), 401-413.

Phumman, P., Niamlang, S., and Sirivat, A. (2009) Fabrication of poly(p-Phenylene)/zeolite composites and their responses towards ammonia. Sensors, 9(10), 8031-8046.

Ragupathy, D., Gopalan, A., and Lee, K.P. (2009) Layer-by-layer electrochemical assembly of poly(diphenylamine)/phosphotungstic acid as ascorbic acid sensor. Microchimica Acta, 166(3), 303-310.

Sahner, K., Hagen, G., Schönauer, D., Reiß, S., and Moos, R. (2008) Zeolites — versatile materials for gas sensors. Solid State Ionics, 179(40), 2416-2423.

Saidina, A.N.A. and Anggoro, D.D. (2002) Dealuminated ZSM-5 zeolite catalyst for ethylene oligomerization to liquid fuels. Journal of Natural Gas Chemistry, 11(1), 79-86.

Santhosh, P., Manesh, K.M., Gopalan, A., and Lee, K.P. (2007) Novel amperometric carbon monoxide sensor based on multi-wall carbon nanotubes grafted with polydiphenylamine—fabrication and performance. Sensors and Actuators B: Chemical, 125(1), 92-99.

Sathiyanarayanan, S., Muthukrishnan, S., and Venkatachari, G. (2006) Synthesis and anticorrosion properties of polydiphenylamine blended vinyl coatings. Synthetic Metals, 156(18–20), 1208-1212.

Shamloo, A., Vosoughi, M., Alemzadeh, I., Naeini, A.T., and Darvish, M. (2012) Two nano structured polymers: polyaniline nanofibers and new linear-dendritic matrix of poly(Citric Acid)-block-poly(ethylene glycol) copolymers for environmental monitoring in novel biosensors. International Journal of Polymeric Materials, 62(7), 377-383.

Shirazi, L., Jamshidi, E., and Ghasemi, M.R. (2008) The effect of Si/Al ratio of ZSM-5 zeolite on its morphology, acidity and crystal size. Crystal Research and Technology, 43(12), 1300-1306.

Shough, A.M. (2008) Quantum chemistry studies of catalytic and photocatalytic materials: transition metal substitution, active sites, thermodynamics and reaction mechanisms. Ph.D. Dissertation, University of Delaware, Newark, DE, USA.

Shukla, P., Bhatia, V., Gaur, V., and Jain, V.K. (2011) Electrostatically functionalized multiwalled carbon nanotube/PMMA composite thin films for organic vapor detection. Polymer-Plastics Technology and Engineering, 50(11), 1179-1184.

Sidebottom, H. and Franklin, J. (1996) The atmospheric fate and impact of hydrochlorofluorocarbons and chlorinated solvents. Pure and Applied Chemistry, 68(9), 1757-1769.

Silverstein, R.M., Webster, F.X., and Kiemle, D. (2005) Spectrometric Identification of Organic Compounds. New York: John Willey.

Suganandam, K., Santhosh, P., Sankarasubramanian, M., Gopalan, A., Vasudevan, T., and Lee, K.P. (2005) Fe^{3+} ion sensing characteristics of polydiphenylamine—electrochemical and spectroelectrochemical analysis. Sensors and Actuators B: Chemical, 105(2), 223-231.

Thuwachaowsoan, K., Chotpattananont, D., Sirivat, A., Rujiravanit, R., and Schwank, J.W. (2007) Electrical conductivity responses and interactions of poly(3-thiopheneacetic acid)/zeolites L, mordenite, beta and H_2. Materials Science and Engineering: B, 140(1–2), 23-30.

Titova, T.I., Kosheleva, L.S., Zhdanov, S.P., and Shubaeva, M.A. (1993) IR spectroscopic study of structure-chemical aspects of the Na-Y zeolite

dealumination with ethylene diamine tetraacetic acid. Pure and Applied Chemistry, 65(10), 2231-2236.

Triantafillidis C.S., Vlessidis A.G., and Evmiridis, N.P. (2000) Dealuminated H-Y zeolites : Influence of the degree and the type of dealumination method on the structural and acidic characteristics of H-Y zeolites. Industrial & Engineering Chemistry Research, 39(2), 307-319.

Tsai, Y.T., Wen, T.C., and Gopalan, A. (2003) Tuning the optical sensing of pH by poly(diphenylamine). Sensors and Actuators B: Chemical, 96(3), 646-657.

Valkenberg, M.H. and Holderich, W.F. (2002) Preparation and use of hybrid organic-inorganic catalysts. Catalysis Reviews-Science and Engineering, 44(2), 321-374.

Vijayakumar, N., Subramanian, E., and Padiyan, D.P. (2012) Conducting polyaniline blends with the soft template poly(Vinyl Pyrrolidone) and their chemosensor application. International Journal of Polymeric Materials, 61(11), 847-863.

Xia, Y., Liu, S., Wang, X., Han, Y., Li, J., and Jian, X. (2008) The analysis of synergistic effects of zeolites applied in intumescent halogen-free flame-retardant ABS composites. Polymer-Plastics Technology and Engineering, 47(6), 613-618.

Xie, H., Yang, Q.D., Sun, X., Yu, T., Huang, J.Z., and Huang, Y. (2005) Gas sensors based on nanosized-zeolite films to identify dimethylmethylphosphonate. Sensors and Materials, 17(1), 21-28.

Xu, L., Hu, X., Tze Lim, Y., and Subramanian, V.S. (2002) Organic vapor adsorption behavior of poly(3-butoxythiophene) LB films on quartz crystal microbalance. Thin Solid Films, 417(1–2), 90-94.

Zhao, Y., Chen, M., Liu, X., Xu, T., and Liu, W. (2005) Electrochemical synthesis of polydiphenylamine nanofibrils through AAO template. Materials Chemistry and Physics, 91(2–3), 518-523.

Zheng, Y., Li, X., and Dutta, P.K. (2012) Exploitation of unique properties of zeolites in the development of gas sensors. Sensors, 12(4), 5170-5194.

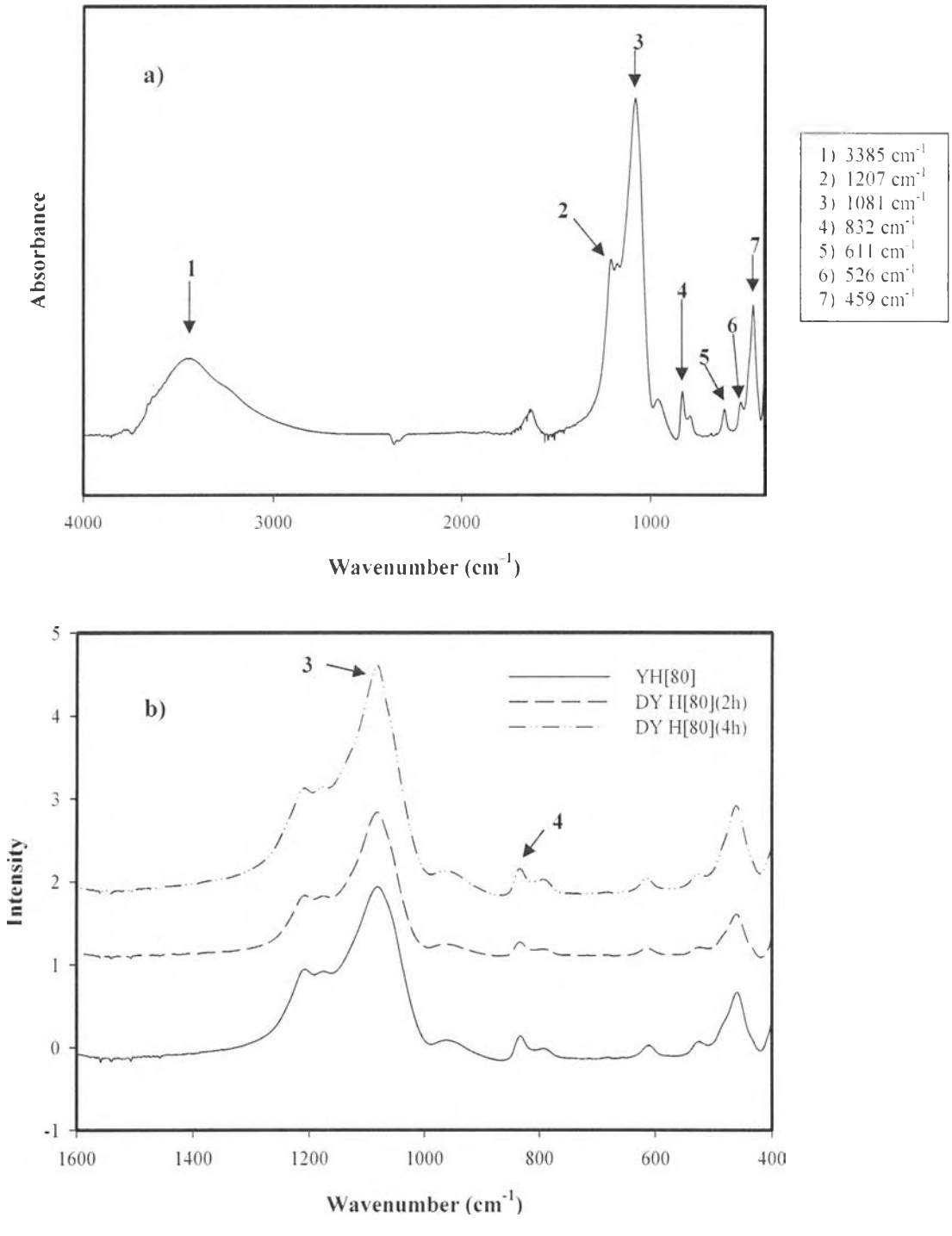

Figure 4.1 FT-IR spectra of: a) YH[80]; and b) DYH[80].

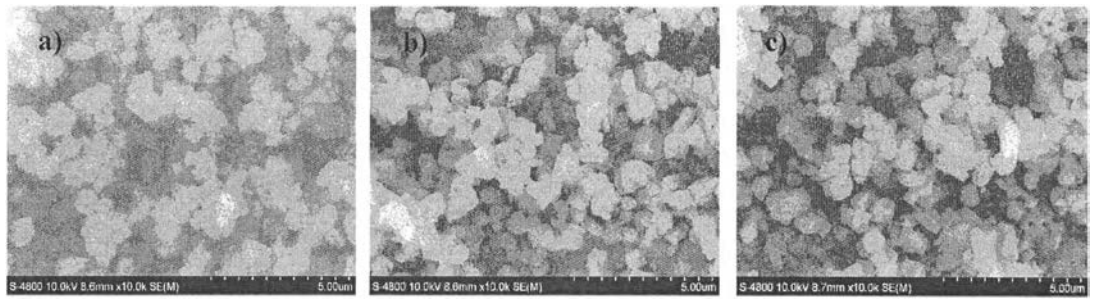

Figure 4.2 Scanning electron micrographs of dealuminated zeolite with different acid treatment times: a) 0 hr; b) 2 hr; and c) 4 hr.

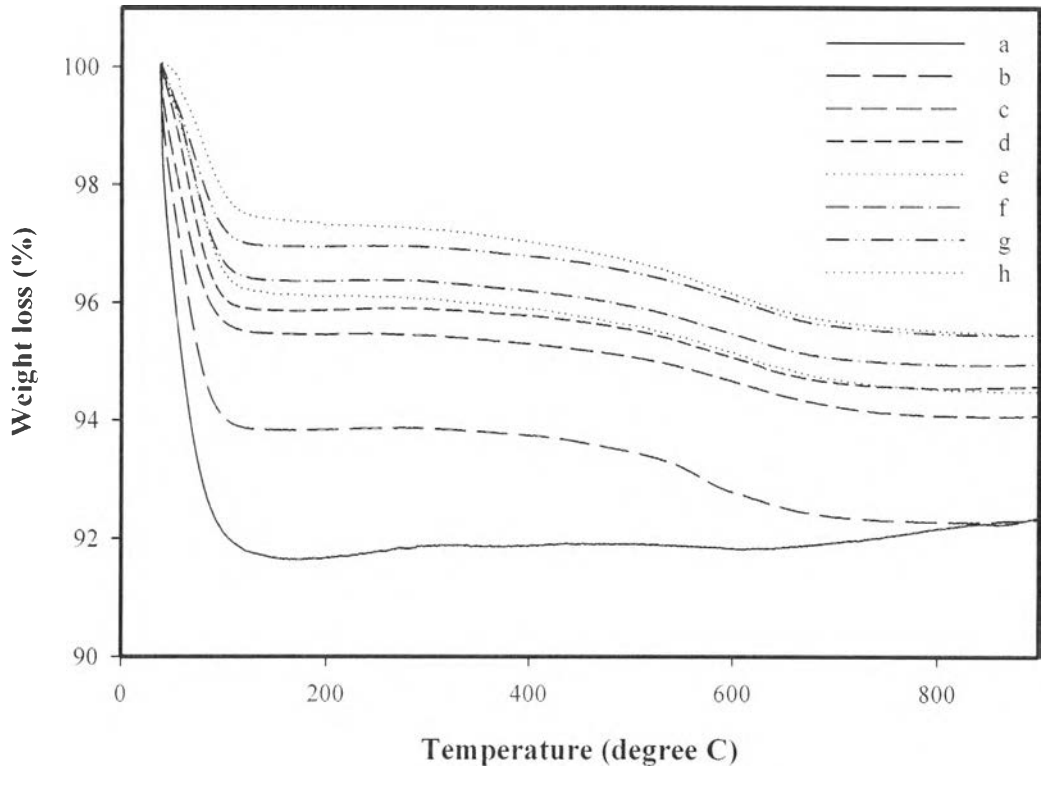

Figure 4.3 TGA thermogram of dealuminated zeolite Y as various treatment times: a) 0 hr; b) 2 hr; c) 4 hr; d) 8 hr; e) 10 hr; f) 12 hr; g) 18 hr; and h) 24 hr.

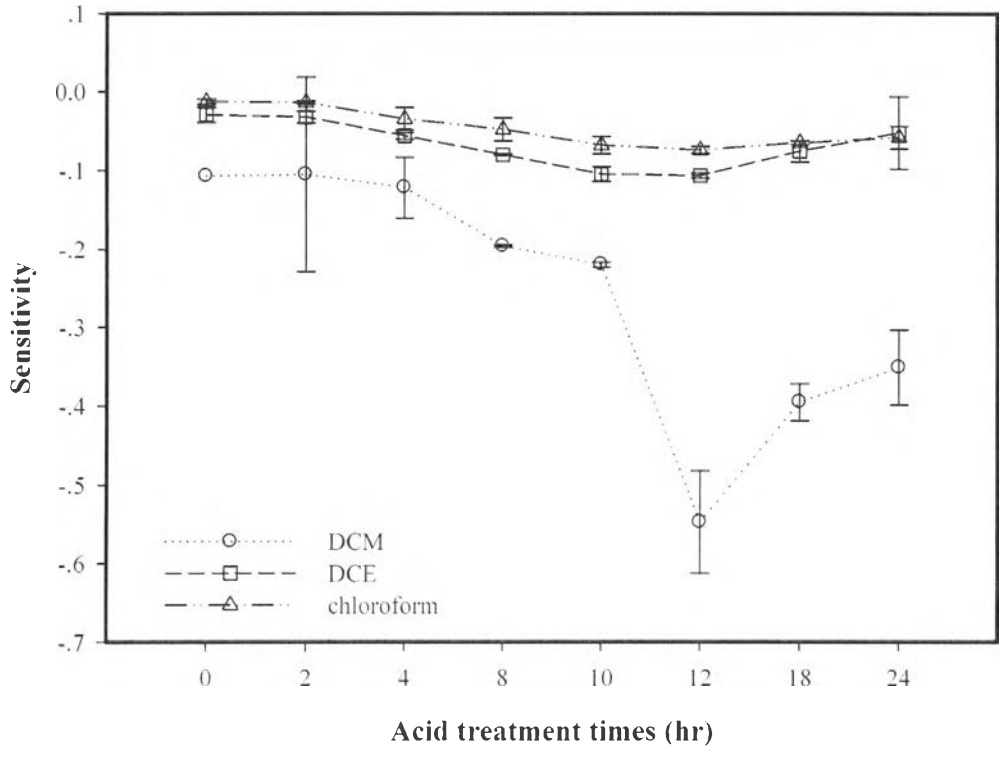

Figure 4.4 Sensitivity of dealuminated zeolite Y at various acid treatment times towards dichloromethane (DCM), 1, 2-dichloroethane (DCE), chloroform.

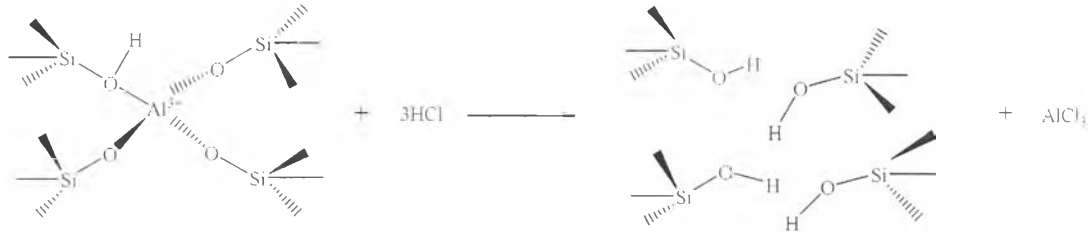

Figure 4.5 Mechanism of silanols during dealumination in HCl medium.

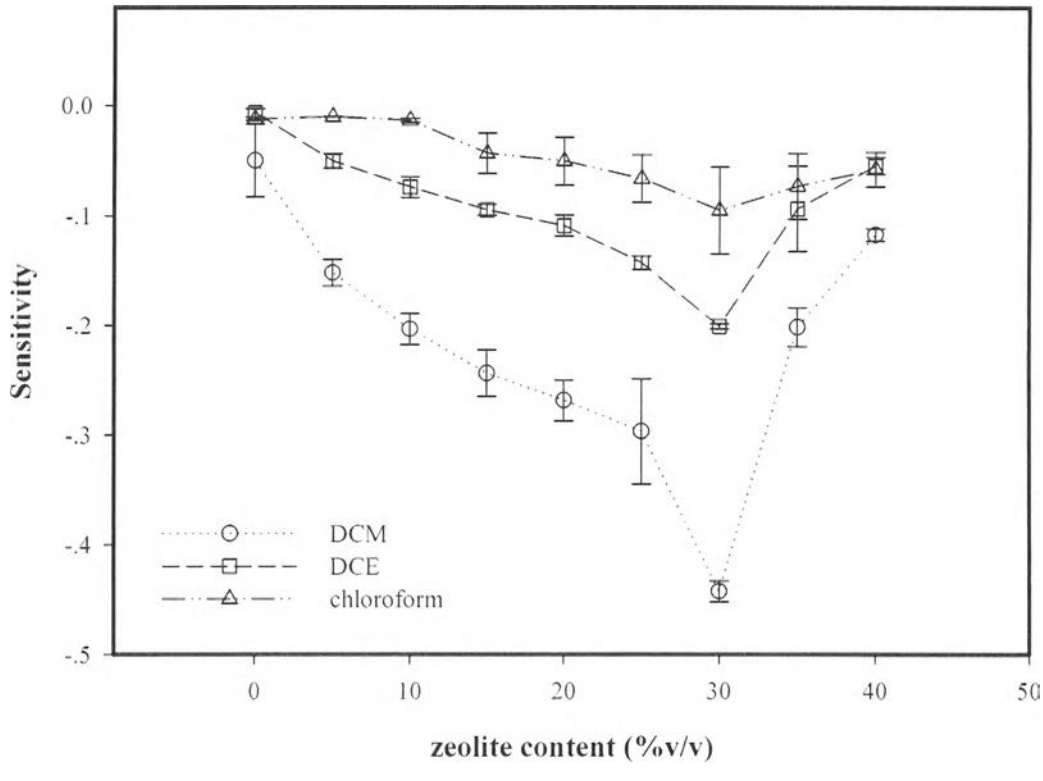

Figure 4.6 Sensitivity of D-PDPA/DYH[80](12h) composites at various zeolite contents towards dichloromethane (DCM), 1, 2-dichloroethane (DCE), chloroform.

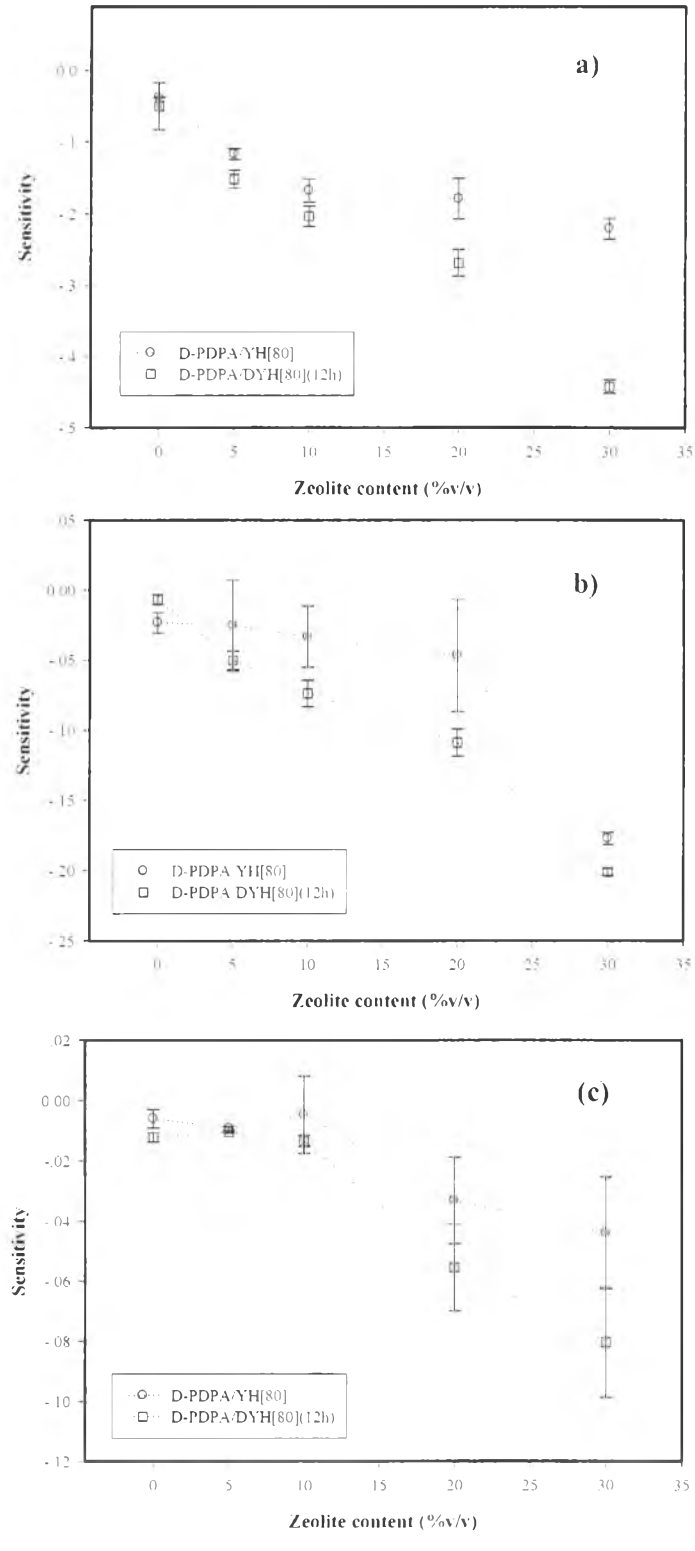

Figure 4.7 Sensitivity of composite with YH[80] and DYH[80](12h) towards: (a) DCM; (b) DCE; and (c) chloroform.

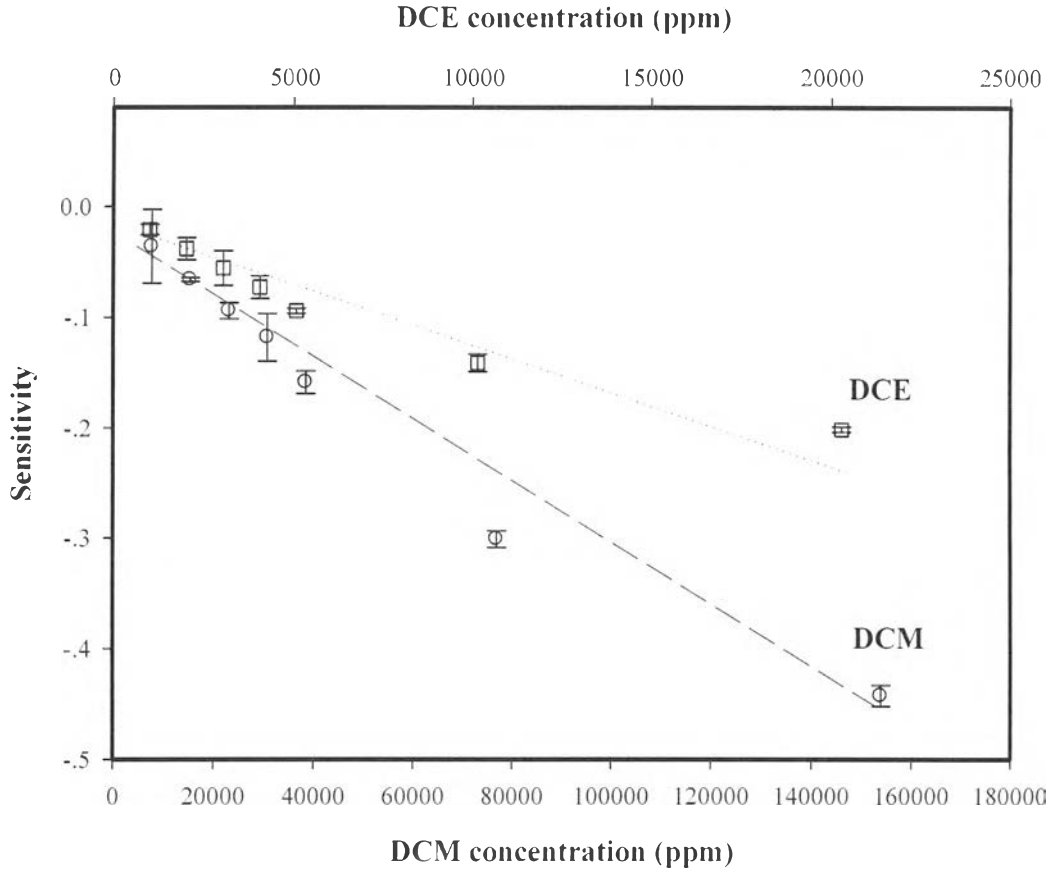

Figure 4.8 The sensitivity of D-PDPA/DYH[80](12h) composite toward DCM and DCE at different concentrations at 27 ± 1 °C and 1 atm.

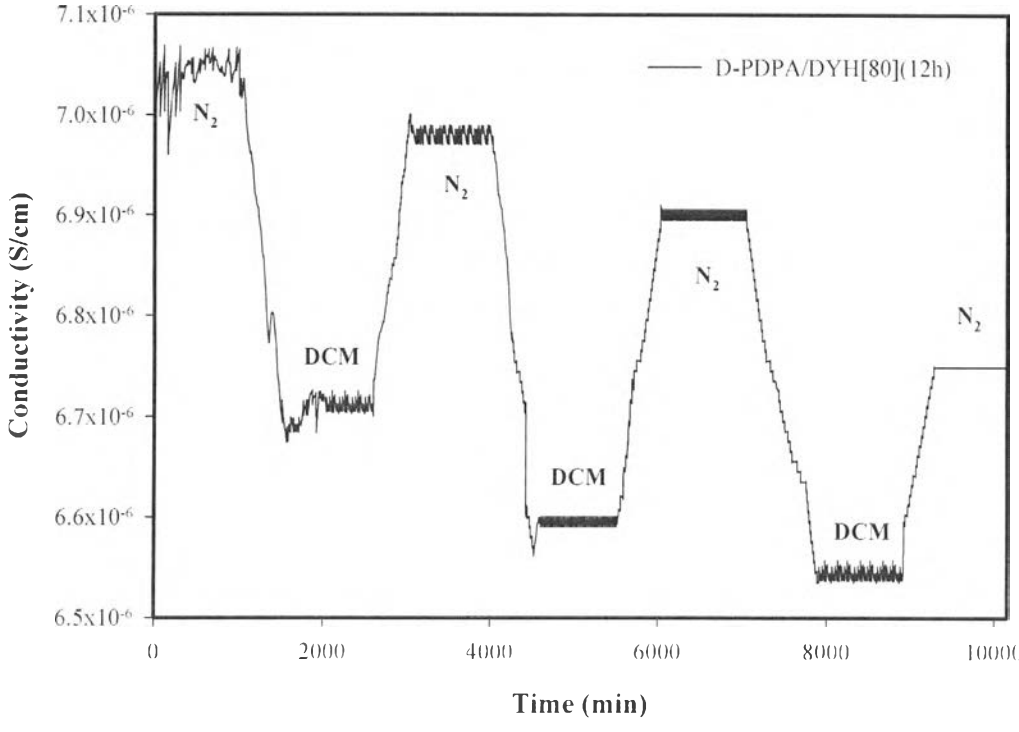

Figure 4.9 Negative cyclic responses of D-PDPA/DYH[80](12h) composite exposed to 50 %v/v DCM vapor at 27 °C. 70 %RH.

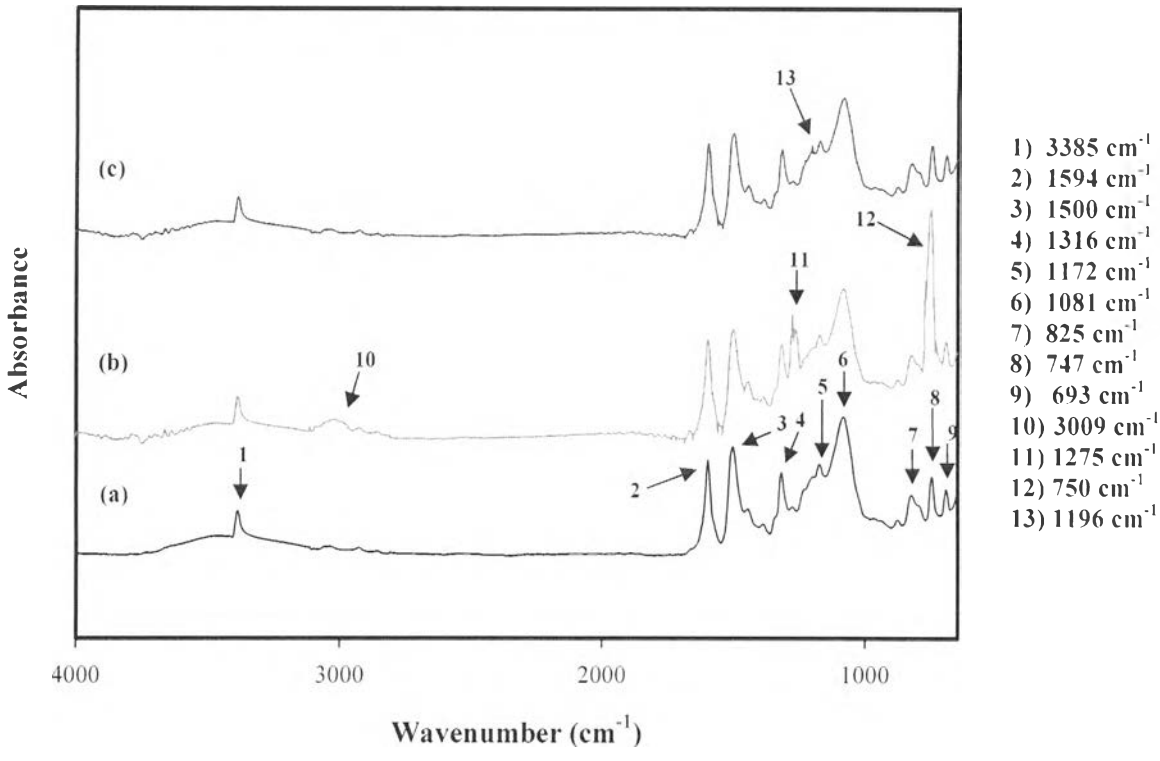

Figure 4.10 FT-IR spectra of D-PDPA/DYH[80](12h) composite exposed to 50%v/v DCM vapors at 27 °C, 70 %RH: (a) before DCM exposure; (b) during DCM exposure; (c) after DCM exposure.

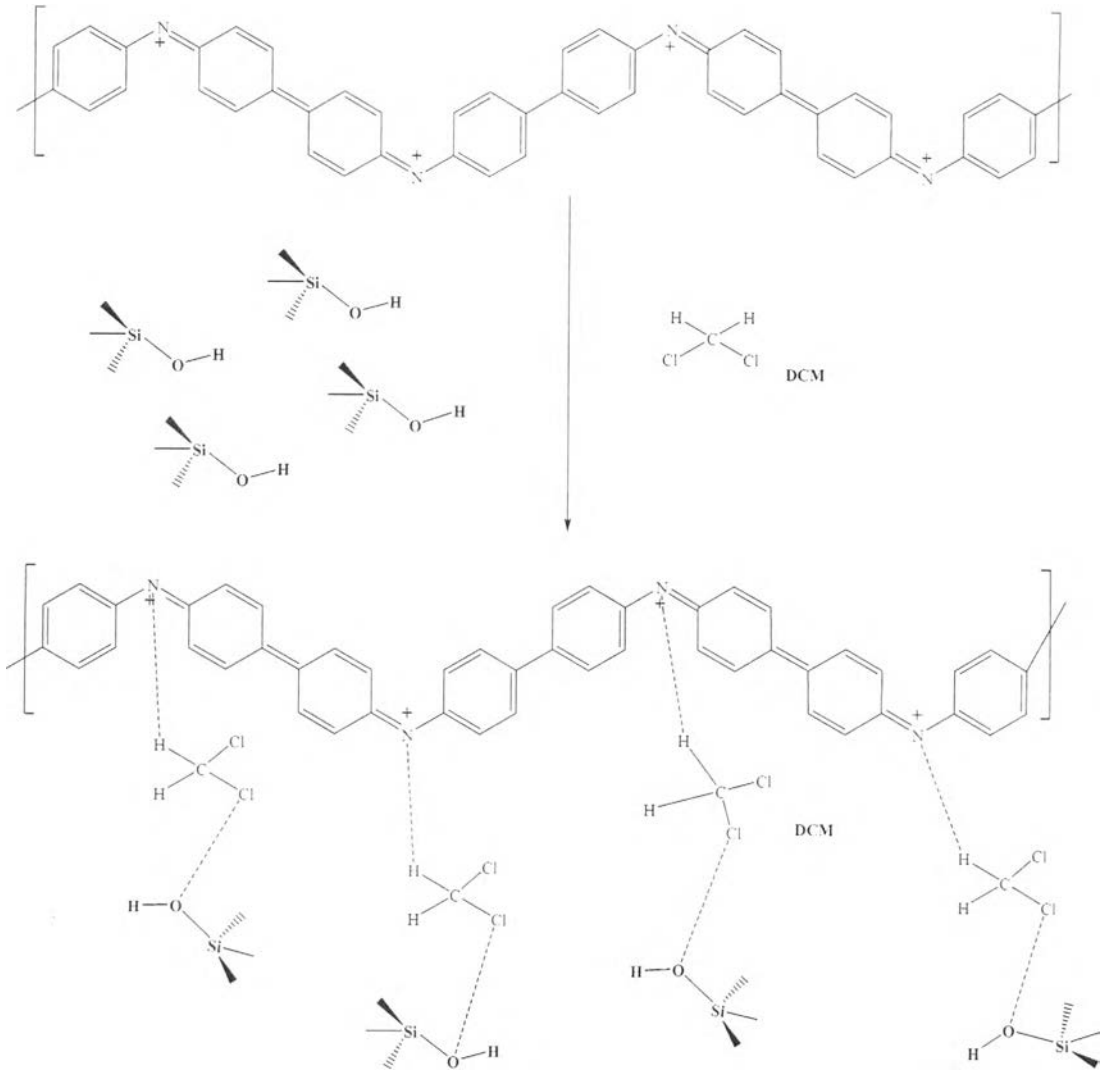

Figure 4.11 Proposed mechanism for the interactions of D-PDPA/DYH[80](12h) composite and DCM vapor.

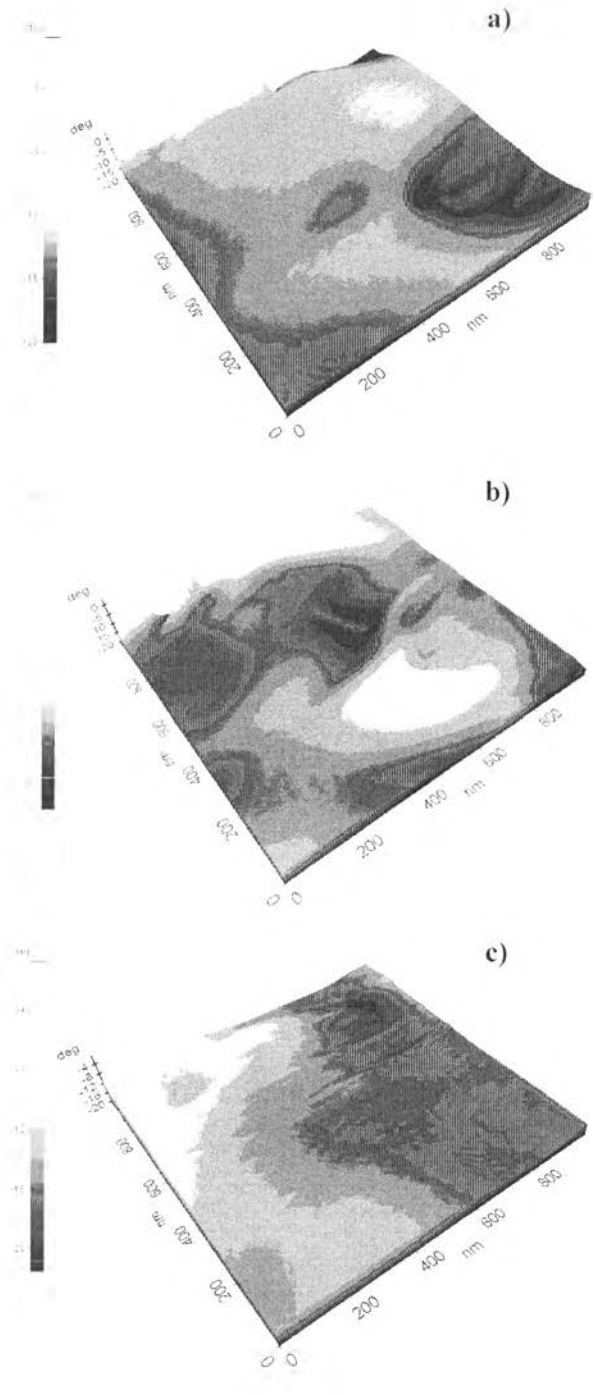

Figure 4.12 EFM images of D-PDPA/DYH[80](12h) composite: a) before; b) during: and c) after exposed to DCM vapor.

Table 4.1 Properties of dealuminated zeolite Y

Zeolite	Acid treatment time (hr)	Integrated band area (cm^{-1})	Si/Al ratio	Surface area (m^2/g)	Crystal size (μm)
YH[80]	0	164.32 ± 6.07	61.58 ± 1.95	683.78 ± 13.32	1.138 ± 0.178
DYH[80](2h)	2	100.62 ± 0.40	131.98 ± 1.57	709.39 ± 9.65	1.029 ± 0.105
DYH[80](4h)	4	43.17 ± 0.20	135.62 ± 1.97	749.85 ± 54.66	0.899 ± 0.088
DYH[80](8h)	8	36.48 ± 0.16	137.48 ± 2.51	754.85 ± 54.66	0.788 ± 0.057
DYH[80](10h)	10	20.68 ± 6.22	197.22 ± 3.84	837.20 ± 0.71	0.708 ± 0.068
DYH[80](12h)	12	16.67 ± 0.77	263.34 ± 2.40	930.58 ± 0.03	0.670 ± 0.057
DYH[80](18h)	18	17.26 ± 5.56	172.81 ± 4.12	580.90 ± 13.87	0.665 ± 0.036
DYH[80](24h)	24	14.20 ± 0.17	142.73 ± 1.35	542.10 ± 26.73	0.614 ± 0.086

Table 4.2 The electrical response ($\Delta\sigma$), sensitivity ($\Delta\sigma/\sigma i$) of YH[80], and DYH[80] when exposed to halogenated solvents (Measurements were made under chamber temperature of 27 ± 1 °C at atmospheric pressure)

Materials	Response ($\Delta\sigma = \sigma_{halogenated\ solvent} - \sigma_{N2}$)			Sensitivity ($\Delta\sigma/\Delta\sigma_{N2}$)		
	DCM	DCE	Chloroform	DCM	DCE	Chloroform
YH[80]	$(-5.06 \pm 2.29)\times10^{-6}$	$(-5.01 \pm 2.57)\times10^{-7}$	$(-4.17 \pm 3.40)\times10^{-7}$	$(-1.20 \pm 0.44)\times10^{-1}$	$(-6.27 \pm 0.71)\times10^{-2}$	$(-7.13 \pm 0.34)\times10^{-2}$
DYH[80](2h)	$(-5.75 \pm 4.96)\times10^{-7}$	$(-2.12 \pm 1.92)\times10^{-7}$	$(-9.12 \pm 5.45)\times10^{-8}$	$(-1.21 \pm 0.90)\times10^{-1}$	$(-3.30 \pm 0.75)\times10^{-2}$	$(-1.37 \pm 0.19)\times10^{-2}$
DYH[80](4h)	$(-1.23 \pm 0.71)\times10^{-6}$	$(-2.99 \pm 0.89)\times10^{-8}$	$(-1.47 \pm 1.23)\times10^{-7}$	$(-1.32 \pm 0.46)\times10^{-1}$	$(-5.65 \pm 0.44)\times10^{-2}$	$(-3.32 \pm 1.43)\times10^{-2}$
DYH[80](8h)	$(-1.94 \pm 0.06)\times10^{-6}$	$(-5.96 \pm 2.57)\times10^{-7}$	$(-2.74 \pm 1.45)\times10^{-7}$	$(-1.96 \pm 0.01)\times10^{-1}$	$(-8.02 \pm 0.09)\times10^{-2}$	$(-4.96 \pm 1.47)\times10^{-2}$
DYH[80](10h)	$(-9.00 \pm 2.08)\times10^{-7}$	$(-6.15 \pm 1.26)\times10^{-7}$	$(-4.03 \pm 0.81)\times10^{-7}$	$(-2.20 \pm 0.03)\times10^{-1}$	$(-9.93 \pm 0.94)\times10^{-2}$	$(-6.35 \pm 1.09)\times10^{-2}$
DYH[80](12h)	$(-7.82 \pm 3.20)\times10^{-6}$	$(-6.95 \pm 0.17)\times10^{-7}$	$(-7.11 \pm 0.55)\times10^{-7}$	$(-5.63 \pm 3.45)\times10^{-1}$	$(-1.07 \pm 0.03)\times10^{-1}$	$(-7.29 \pm 0.44)\times10^{-2}$
DYH[80](18h)	$(-2.18 \pm 0.61)\times10^{-6}$	$(-4.19 \pm 0.73)\times10^{-7}$	$(-3.89 \pm 1.35)\times10^{-7}$	$(-3.91 \pm 0.24)\times10^{-1}$	$(-7.30 \pm 1.37)\times10^{-2}$	$(-6.46 \pm 0.19)\times10^{-2}$
DYH[80](24h)	$(-4.09 \pm 2.25)\times10^{-6}$	$(-7.97 \pm 9.04)\times10^{-7}$	$(-3.27 \pm 0.83)\times10^{-7}$	$(-3.62 \pm 0.48)\times10^{-1}$	$(-6.41 \pm 4.59)\times10^{-2}$	$(-5.79 \pm 1.45)\times10^{-2}$

Table 4.3 The electrical response ($\Delta\sigma$), sensitivity ($\Delta\sigma/\sigma_{N2}$) of D-PDPA and the composite when exposed to halogenated solvents (Measurements were made under chamber temperature of 27 ± 1 °C at atmospheric pressure)

Materials	Response ($\Delta\sigma = \sigma_{\text{halogenated solvent}} - \sigma_{N2}$)			Sensitivity ($\Delta\sigma/\sigma_{N2}$)		
	DCM	DCE	Chloroform	DCM	DCE	Chloroform
D-PDPA	$(-3.13 \pm 2.49)\times10^{-7}$	$(-3.48 \pm 1.17)\times10^{-8}$	$(-1.00 \pm 0.06)\times10^{-7}$	$(-5.30 \pm 3.30)\times10^{-2}$	$(-6.26 \pm 3.70)\times10^{-2}$	$(-1.22 \pm 0.16)\times10^{-3}$
D-PDPA/ 5%DYH[80](12h)	$(-8.43 \pm 0.66)\times10^{-7}$	$(-1.89 \pm 0.66)\times10^{-7}$	$(-9.13 \pm 1.92)\times10^{-8}$	$(-1.51 \pm 0.12)\times10^{-1}$	$(-4.87 \pm 0.65)\times10^{-2}$	$(-1.04 \pm 0.03)\times10^{-2}$
D-PDPA/ 10%DYH[80](12h)	$(-1.26 \pm 1.10)\times10^{-6}$	$(-2.18 \pm 0.49)\times10^{-7}$	$(-1.44 \pm 0.36)\times10^{-7}$	$(-2.09 \pm 0.14)\times10^{-1}$	$(-7.46 \pm 0.95)\times10^{-2}$	$(-1.32 \pm 0.18)\times10^{-2}$
D-PDPA/ 15%DYH[80](12h)	$(-1.21 \pm 0.20)\times10^{-6}$	$(-3.29 \pm 0.17)\times10^{-7}$	$(-3.98 \pm 2.91)\times10^{-7}$	$(-2.15 \pm 0.21)\times10^{-1}$	$(-9.45 \pm 0.50)\times10^{-2}$	$(-4.67 \pm 1.82)\times10^{-2}$
D-PDPA/ 20%DYH[80](12h)	$(-1.42 \pm 0.94)\times10^{-6}$	$(-3.74 \pm 0.91)\times10^{-7}$	$(-2.38 \pm 1.67)\times10^{-7}$	$(-2.62 \pm 0.19)\times10^{-1}$	$(-1.10 \pm 0.96)\times10^{-1}$	$(-5.41 \pm 2.16)\times10^{-2}$
D-PDPA/ 25%DYH[80](12h)	$(-1.15 \pm 0.23)\times10^{-6}$	$(-1.02 \pm 0.82)\times10^{-6}$	$(-3.43 \pm 1.84)\times10^{-7}$	$(-2.88 \pm 0.48)\times10^{-1}$	$(-1.41 \pm 0.06)\times10^{-1}$	$(-6.89 \pm 2.16)\times10^{-2}$
D-PDPA/ 30%DYH[80](12h)	$(-3.04 \pm 1.32)\times10^{-6}$	$(-1.10 \pm 0.20)\times10^{-6}$	$(-5.62 \pm 1.04)\times10^{-7}$	$(-4.44 \pm 0.10)\times10^{-1}$	$(-2.01 \pm 0.25)\times10^{-1}$	$(-9.07 \pm 3.95)\times10^{-2}$
D-PDPA/ 35%DYH[80](12h)	$(-6.28 \pm 2.26)\times10^{-7}$	$(-3.31 \pm 0.13)\times10^{-7}$	$(-2.83 \pm 1.53)\times10^{-7}$	$(-2.04 \pm 0.18)\times10^{-1}$	$(-8.64 \pm 3.88)\times10^{-2}$	$(-7.58 \pm 2.98)\times10^{-2}$
D-PDPA/ 40%DYH[80](12h)	$(-4.49 \pm 1.98)\times10^{-7}$	$(-2.18 \pm 0.57)\times10^{-7}$	$(-1.84 \pm 1.14)\times10^{-7}$	$(-1.19 \pm 0.06)\times10^{-1}$	$(-5.54 \pm 0.77)\times10^{-2}$	$(-5.83 \pm 1.57)\times10^{-2}$

Table 4.4 The induction time (t_i) and the recovery time (t_r) of D-PDPA, YH[80], D-PDPA and DYH[80] composites when exposed to halogenated solvents (Measurements were made under chamber temperature of 27 ± 1 °C at atmospheric pressure)

Materials	t_i (min)			t_r (min)		
	DCM	DCE	Chloroform	DCM	DCE	Chloroform
YH[80]	15.42 ± 0.11	9.45 ± 0.14	6.45 ± 0.57	9.40 ± 0.07	8.69 ± 0.23	8.02 ± 0.46
DYH[80](2h)	14.62 ± 0.23	9.35 ± 0.42	7.40 ± 0.21	7.59 ± 0.12	7.50 ± 0.37	8.46 ± 0.26
DYH[80](4h)	14.93 ± 0.07	10.17 ± 0.07	8.03 ± 0.18	7.63 ± 0.18	8.11 ± 0.18	9.83 ± 0.40
DYH[80](8h)	15.67 ± 0.04	10.29 ± 0.36	8.60 ± 0.53	8.44 ± 0.07	8.46 ± 0.30	10.05 ± 0.16
DYH[80](10h)	15.77 ± 0.17	11.44 ± 0.45	9.01 ± 0.32	8.75 ± 0.07	9.82 ± 0.23	10.17 ± 0.23
DYH[80](12h)	17.61 ± 0.09	12.51 ± 0.23	10.33 ± 0.46	8.88 ± 0.04	9.33 ± 0.48	11.24 ± 0.21
DYH[80](18h)	15.54 ± 0.05	11.78 ± 0.18	10.17 ± 0.25	8.82 ± 0.23	9.23 ± 0.16	9.72 ± 0.30
DYH[80](24h)	15.56 ± 0.01	11.25 ± 0.29	9.48 ± 0.25	9.03 ± 0.18	8.40 ± 0.23	9.40 ± 0.24
D-PDPA 100:1	11.35 ± 0.21	8.01 ± 0.63	7.74 ± 0.34	9.55 ± 0.14	6.83 ± 0.41	6.65 ± 0.28
D-PDPA/ 5%DYH[80](12h)	12.48 ± 0.04	10.48 ± 0.25	10.17 ± 0.07	10.43 ± 0.04	10.87 ± 0.16	10.76 ± 0.16
D-PDPA/ 10%DYH[80](12h)	12.56 ± 0.16	10.89 ± 0.15	10.60 ± 0.23	10.65 ± 0.14	11.15 ± 0.10	11.50 ± 0.16
D-PDPA/ 15%DYH[80](12h)	13.51 ± 0.08	11.38 ± 0.04	11.55 ± 0.28	11.50 ± 0.07	11.50 ± 0.22	12.34 ± 0.23
D-PDPA/ 20%DYH[80](12h)	13.56 ± 0.31	11.71 ± 0.23	12.50 ± 0.22	11.70 ± 0.07	11.72 ± 0.22	12.76 ± 0.16

Table 4.4 The induction time (t_i) and the recovery time (t_r) of D-PDPA, YH[80], D-PDPA and DYH[80] composites when exposed to halogenated solvents (Measurements were made under chamber temperature of 27 ± 1 °C at atmospheric pressure) (cont.)

Materials	t_i (min)			t_r (min)		
	DCM	DCE	Chloroform	DCM	DCE	Chloroform
D-PDPA/ 25%DYH[80](12h)	14.80 ± 0.07	12.17 ± 0.21	13.38 ± 0.23	12.60 ± 0.71	12.02 ± 0.05	12.93 ± 0.52
D-PDPA/ 30%DYH[80](12h)	15.50 ± 0.07	12.81 ± 0.23	13.66 ± 0.30	12.81 ± 0.08	12.39 ± 0.07	13.53 ± 0.07
D-PDPA/ 35%DYH[80](12h)	14.75 ± 0.42	12.51 ± 0.23	13.44 ± 0.30	12.29 ± 0.23	12.66 ± 0.17	13.39 ± 0.52
D-PDPA/ 40%DYH[80](12h)	14.45 ± 0.16	11.67 ± 0.16	12.77 ± 0.17	11.20 ± 0.23	12.82 ± 0.09	12.38 ± 0.07